DISPERSIVE WAVE ATTENUATION DUE TO OROGRAPHIC FORCING*

JUAN CARLOS MUÑOZ GRAJALES† AND ANDRÉ NACHBIN‡

Abstract. The O'Doherty-Anstey approximation (ODA) was originally formulated in the seismological literature for acoustic pulse propagation through a disordered stratified medium. It explains the mechanism for amplitude attenuation (and pulse shaping) promoted by the, variable coefficient, conservative hyperbolic model. This work generalizes the one-dimensional ODA theory for linear weakly dispersive water waves forced by a disordered orography. The analysis is performed through the recently formulated terrain-following Boussinesq system. This is achieved by applying the invariant imbedding method. As a result dispersion alters the medium's correlation function which controls the apparent attenuation mechanism. On the other hand, orography affects the dispersive mechanism for the Airy function-like formation. A nonlinear Boussinesq solver was implemented and theoretical results were validated for different values of the parameters of interest. The theoretical results are in very good agreement with the small amplitude simulations. In particular, the approximate theory was able to capture a good part of the forward scattering radiation. Moreover, through numerical experiments the theory is pushed beyond its expected regime and captures the attenuation of small amplitude solitons due to orographic forcing.

Key words. dispersive waves, inhomogeneous media, asymptotic theory

AMS subject classifications. 76B07, 76B15, 35Q

1. Introduction.

Wave–topography interaction has been the subject of considerable mathematical research. The physical applications range from coastal surface waves [13] to atmospheric flows over mountain ranges [2, 6]. In particular, the interaction of waves with fine features of the topography is of great interest. As pointed out in the introduction to the *Orography* proceedings [6] of the European Centre for Medium-Range Weather Forecasts (ECMWF), the "representation (...) of subgrid-scale orographic processes is recognized as crucial to numerical weather prediction at all time ranges". In the atmospheric literature *orography* implies mountain ranges [2]. Our study is therefore focused on the effect of small-scale orographic features, which we call the *microstructure*. A mathematical theory is described and its robustness validated numerically. As surface gravity waves propagate from deep to shallow waters, they are transformed due to shoaling, refraction, diffraction and reflection. In order to concentrate on the main scattering mechanism connected with the pulse shaping phenomenon to be described, we consider the normal incidence of surface pulse shaped waves. These waves propagate over topographies containing a smooth slowly varying profile together with disordered small-scale features. As pointed out, our goal is to capture the wave-microstructure interaction.

The main result is that the disordered medium fluctuations cause the propagating pulse to broaden as it travels. Due to multiple scattered energy, the pulse appears to diffuse about a moving center. The amount of broadening and attenuation is proportional to the traveling distance and depends on the disorder's correlation function. In the sequel we refer to the transformation of the pulse, due to the medium's microscale fluctuations as *pulse shaping*.

*This work was supported by CNPq/Brazil under Grant 300368/96-8.

†Instituto de Matemática Pura e Aplicada, Est. D. Castorina 110, Jardim Botânico, Rio de Janeiro, RJ 22460-320, Brazil (juanc@impa.br).

‡Instituto de Matemática Pura e Aplicada, Est. D. Castorina 110, Jardim Botânico, Rio de Janeiro, RJ 22460-320, Brazil (nachbin@impa.br).

The theory for pulse shaping was originally derived in the context of acoustic wave propagation in the earth's crust [20]. It is known as the O'Doherty–Anstey (ODA) approximation. In the acoustic wave applications several authors have analyzed the spreading of a pulse due to the microscale variations in the medium parameters (c.f. for example the work by Clouet and Fouque [8], Papanicolaou and Sølna [22] and Lewicki *et al.* [10]). The motivation for modeling in terms of a random medium is that a detailed description of microscale medium fluctuations are often not known. Using a stochastic model uncertainties about a specific medium are translated into uncertainties about a transmitted pulse shape in a systematic way [1]. Stochastic modeling has been used by one of the authors for long, weakly dispersive surface wave problems [17, 19].

This work generalizes the one-dimensional ODA theory for linear weakly dispersive water waves, when forced by a disordered orography. The analysis is performed through the recently formulated terrain-following Boussinesq system [18]. This is achieved by applying the invariant imbedding method. As a result dispersion alters the medium's correlation function which controls the apparent attenuation mechanism. On the other hand, orography affects the dispersive mechanism for the Airy function-like formation. A nonlinear Boussinesq solver was implemented and theoretical results were validated for different values of the parameters of interest. Details of the numerical method and a larger range of experiments are presented elsewhere [15]. The theoretical results presented here are in very good agreement with the small amplitude simulations. This amounts to solving the nonlinear Boussinesq system with data on a small amplitude-to-depth ratio. In particular, the approximate theory was able to capture a good part of the forward scattering radiation.

This paper is organized as follows. In section 2 we present the terrain-following Boussinesq system. In section 3 the pulse shaping (ODA) theory is formulated in detail. Section 4 contains five sets of numerical experiments validating the theory and generating further insight into the theory. The conclusions are given in section 5. A three part appendix is intended to provide further detail to the reader.

2. The linearized terrain-following Boussinesq model. In past years Boussinesq-type equations have been employed to model surface waves propagation in shallow channels. In such models the fluid is assumed to be inviscid, incompressible and irrotational. Peregrine [21] in 1967 deduced a model valid for channels of slowly varying depth, whereas Hamilton [9] in 1977 derived a set of equations valid for arbitrary orographies. He used an appropriate curvilinear coordinate system and applied a perturbation approach to the linear potential theory equations retaining the lowest-order effects of dispersion. Hamilton also outlines the formulation of a weakly nonlinear model by considering a Langragian functional. Using dimensionless variables and Hamilton's conformal mapping strategy, Nachbin [18] derived the nonlinear terrain-following Boussinesq system

$$
\begin{aligned}
M(\xi)\eta_t + \left(\left(1+\frac{\alpha\eta}{M(\xi)}\right)u\right)_\xi &= 0,\\
u_t + \eta_\xi + \frac{\alpha}{2}\left(\frac{u^2}{M(\xi)^2}\right)_\xi - \frac{\beta}{3}u_{\xi\xi t} &= 0,
\end{aligned}
$$

where the parameter $\alpha = a_o/h_o$ regulates the strength of nonlinear effects and $\beta = h_o^2/\lambda^2$ the level of dispersion. The characteristic wave amplitude is a_o, the characteristic wavelength is λ and the typical depth is h_o. When $\alpha = 0$ the system above reduces to

$$M(\xi)\eta_t + u_\xi = 0, \qquad (2.1)$$
$$u_t + \eta_\xi - \frac{\beta}{3}u_{\xi\xi t} = 0.$$

Here ξ and t are the space and time coordinates, respectively, $\eta = \eta(\xi,t)$ is the wave elevation and $u = u(\xi,t)$ is the weigthed depth-averaged terrain-following velocity [18]. The variable coefficient $M(\xi)$ is a smooth orography dependent function which appears as a consequence of the changes of variables [18]. When the parameter β is small we are in the shallow channel/long wave regime. Equivalently this is called the weakly dispersive regime.

3. The linear pulse-shaping theory. In this section we generalize the O'Doherty-Anstey (ODA) approximation from linear acoustic waves to the linear weakly dispersive system (2.1). The weakly dispersive Boussinesq system is forced by a rapidly varying orography expressed through the variable coefficient $M(\xi)$. We consider a technique analogous to Berlyand and Burridge's acoustic work [3], which we apply successfully to dispersive waves due to two reasons. First, system (2.1) can be written equivalently as two coupled KdV-type equations for the transmitted and reflected fields. These linearized KdV-type equations can be viewed as a dispersive perturbation to those obtained by Berlyand and Burridge. Namely a propagating pulse will slowly disperse with a given (known) rate (c.f. appendix A, equation (A.4)). Second, the pulse's effective propagation velocity is bounded and all Fourier modes have positive phase speeds bounded by 1. These two properties described allow us to apply the *invariant imbedding approach* [14], taking the propagation distance as the *imbedding parameter*.

In what follows solutions u,η to (2.1) will be assumed to be smooth enough and absolutely integrable. This requirement is necessary to justify the use of the Fourier transform and the Fourier inversion formula.

We start by performing the change of variables

$$x = \int_0^\xi \frac{1}{C_o(s)}ds, \quad t' = t,$$

in system (2.1). Here $C_o(s) = \sqrt{1/M(s)}$ is the *local wave speed* and x is the *travel time*. Dropping the primes system (2.1) becomes

$$C_o^{-1/2}\ \eta_t + C_o^{1/2}\ u_x = 0, \qquad (3.1)$$
$$C_o^{1/2}\ u_t + C_o^{-1/2}\ \eta_x - \frac{\beta}{3C_o^{1/2}}\left(u_{xxt}\ \frac{1}{C_o} + \left(\frac{1}{C_o}\right)_x u_{xt}\right) = 0.$$

We adopt the *wave mode splitting*

$$R = C_o^{1/2}u + C_o^{-1/2}\eta, \qquad (3.2)$$

$$L = -C_o^{1/2}u + C_o^{-1/2}\eta. \qquad (3.3)$$

Differentiating (3.2) and (3.3) with respect to x and t, using (3.1) and the fact that $u = (R-L)/(2C_o^{1/2})$, leads to the coupled wave mode system

$$R_t + R_x = p(x)\left(\frac{R-L}{2C_o^{1/2}}\right)_{xxt} + q(x)\left(\frac{R-L}{2C_o^{1/2}}\right)_{xt} - r(x)L, \qquad (3.4)$$
$$L_x - L_t = p(x)\left(\frac{R-L}{2C_o^{1/2}}\right)_{xxt} + q(x)\left(\frac{R-L}{2C_o^{1/2}}\right)_{xt} - r(x)R,$$

where the variable coefficients are

$$p(x) = \frac{\beta}{3C_o^{3/2}(x)}, \quad q(x) = -\frac{\beta C_{o,x}(x)}{3C_o^{5/2}(x)}, \quad \text{and} \quad r(x) = \frac{C_{o,x}(x)}{2C_o(x)}.$$

The initial conditions for system (3.4) are

$$R(x,0) = R_o(x), \quad L(x,0) = 0.$$

Note that when the bottom is flat ($r \equiv 0$) and $\beta = 0$ (no dispersion) equations (3.4) identify R with a wave propagating to the right (transmitted wave) and L with a wave propagating to the left (reflected wave). For variable depths we adopt the same terminology. Moreover, this terminology is also consistent for system (3.4), in the weakly dispersive regime ($0 < \beta << 1$) and $r \equiv 0$, since the left propagating signal L is negligible if the initial data corresponds to a rightgoing wave (see appendix A).

Several decompositions of the Boussinesq equations into a pair of KdV equations are introduced by Mattioli in [11] and [12]. We point out that system (3.4) has some advantages with respect to those decompositions presented by Mattioli. First, unlike system (3.4), the Boussinesq equations used by Mattioli are not valid as an asymptotic approximation of the potential theory equations for arbitrary rapidly-varying or non-differentiable orographies. Second, in contrast to system (3.4), the linear dispersion relation for Mattioli's model results in unstable short waves with amplitude tending to infinity.

In order to set our forthcoming results in a wave propagating frame let us introduce the change of variables

$$\tau = t - x, \quad x' = x,$$

where τ is the time-delay variable. Again abandoning the primes, equations (3.4) become

$$\begin{aligned} R_x &= p\left(\frac{R-L}{2C_o^{1/2}}\right)_{\tau\tau\tau} - 2p\left(\frac{R-L}{2C_o^{1/2}}\right)_{x\tau\tau} + p\left(\frac{R-L}{2C_o^{1/2}}\right)_{xx\tau} \\ &\quad -q\left(\frac{R-L}{2C_o^{1/2}}\right)_{\tau\tau} + q\left(\frac{R-L}{2C_o^{1/2}}\right)_{x\tau} - rL, \\ L_x - 2L_\tau &= p\left(\frac{R-L}{2C_o^{1/2}}\right)_{\tau\tau\tau} - 2p\left(\frac{R-L}{2C_o^{1/2}}\right)_{x\tau\tau} + p\left(\frac{R-L}{2C_o^{1/2}}\right)_{xx\tau} \\ &\quad -q\left(\frac{R-L}{2C_o^{1/2}}\right)_{\tau\tau} + q\left(\frac{R-L}{2C_o^{1/2}}\right)_{x\tau} - rR. \end{aligned} \tag{3.5}$$

Let $\widehat{f}(\omega)$ denote the Fourier Transform of $f(\tau)$ in the time-delay variable τ:

$$\widehat{f}(\omega) = \int_{-\infty}^{\infty} e^{-i\omega\tau} f(\tau)\, d\tau.$$

Take the Fourier Transform in τ of equations (3.5). Manipulate the resulting system in order to obtain first order equations for the travel time-evolution of the Fourier modes. This goal is achieved by first subtracting the two equations giving

$$\widehat{R}_x - \widehat{L}_x = r\widehat{R} - 2i\omega\widehat{L} - r\widehat{L}. \tag{3.6}$$

Moreover, by differentiating this equation with respect to x we find

$$\widehat{R}_{xx} - \widehat{L}_{xx} = r'(x)\widehat{R} - r'(x)\widehat{L} - 2iw\widehat{R}_x + 2iwr(x)\widehat{R} + 4w^2\widehat{L} - 4iwr(x)\widehat{L} + r^2(x)\widehat{R} - r^2(x)\widehat{L}. \tag{3.7}$$

This expression can be used to eliminate the second order $x-$derivatives in the first Fourier transformed equation arising from (3.5). This is a crucial step in order to apply the invariant imbedding approach, which requires a first order system of ordinary differential equations (ODE). Using the fact that the time frequency range $|\omega| < C_o(x)\sqrt{3/\beta}$ (see appendix A) we solve for $\widehat{R}_x$ to obtain

$$\widehat{R}_x = \zeta(x,\omega)\widehat{L} + \gamma(x,\omega)\widehat{R}, \tag{3.8}$$

where

$$\zeta(x,\omega) = \frac{id(x)\omega^3 + e(x)\omega^2 - 2r(x)}{2(1-d(x)\ \omega^2)}, \quad \gamma(x,\omega) = \frac{\frac{-i\beta\omega^2}{3C_o^2(x)}(\omega - 4ir(x))}{2\left(1 - \frac{\beta\omega^2}{3C_o^2(x)}\right)},$$

$$d(x) = \frac{\beta}{3C_o^2(x)} \quad \text{and} \quad e(x) = -\frac{\beta}{3C_o^3(x)}C_{o,x}(x).$$

Putting equation (3.8) into equation (3.6) and solving for $\widehat{L}_x$ results in

$$\widehat{L}_x = (2i\omega + \bar{\gamma}(x,\omega))\widehat{L} + \bar{\zeta}(x,\omega)\widehat{R}, \tag{3.9}$$

where $\bar{\zeta}(x,w)$ and $\bar{\gamma}(x,w)$ denote the complex conjugates of $\zeta(x,w)$ and $\gamma(x,w)$, respectively. As claimed above, equations (3.8) and (3.9) give the evolution in x (travel time) of each Fourier mode, corresponding to the transmitted and reflected fields.

Next, suppose that we want to calculate $L(x_o,\tau) = L(x_o,\tau;T)$ for $0 \le \tau \le T$. At this step we apply the *invariant imbedding approach* [14] to system (3.8) and (3.9). To do so we imbed the relevant inhomogeneous region inside a homogeneous medium so that we can give appropriate boundary conditions at the border of the medium's slab $[x_o, x_o + X]$, say

$$\widehat{R}(x_o,\omega;T) = \widehat{h}(\omega), \tag{3.10}$$

$$\widehat{L}(x_o + X,\omega;T) = 0. \tag{3.11}$$

Boundary condition (3.11) means that no reflection is expected at the downstream travel time location $x_o{+}X$ when $0 < \tau = t{-}x_o < T$. In other words, the signal did not have enough time to arrive at this point and to produce a medium's response. This is true at least for some $X > 0$ large enough (depending on T) due to the pulse's finite (effective) velocity mentioned earlier. Linearity of ODE system (3.8)-(3.9) and the invariant imbedding technique [14] guarantees the existence of a function $K(x,\omega;T)$ (called the *reflection kernel*) such that

$$\widehat{L}(x,\omega;T) = \widehat{K}(x,\omega;T)\ \widehat{R}(x,\omega;T) \tag{3.12}$$

and satisfying the Ricatti-type equation

$$\widehat{K}_x = \bar{\zeta}(x,\omega) + 2i\omega\Gamma(x,\omega)\widehat{K} - \zeta(x,\omega)\widehat{K}^2, \tag{3.13}$$

with

$$\Gamma(x,\omega) = \frac{2 - d(x)\omega^2}{2(1 - d(x)\omega^2)}.$$

From equation (3.11) we obtain an appropriate initial condition for equation (3.13):

$$\widehat{K}(x_o + X, \omega; T) = 0. \tag{3.14}$$

Notice that equation (3.12) allows us to solve for the reflected signal $L(x_o, \tau; T)$ in terms of the reflection kernel $K(x_o, \tau; T)$ and the transmitted pulse $R(x_o, \tau; T)$ for $0 \leq \tau \leq T$. This function K contains all the information about medium's reflection properties. We also remark that the boundary value problem (3.8), (3.9), (3.10), (3.11) has been reduced to solving the initial value problem (3.13)-(3.14) in reversed direction from the travel time location $x_o + X$ up to the time of interest x_o.

In general it is not possible to solve explicitly for $\widehat{K}$ from equation (3.13) so we adopt an approximation. To this end we present the following generalization to the lemma given by Berlyand and Burridge [3].

LEMMA 3.1. *Let y satisfy the Ricatti equation*

$$y'(s) = -A(s) - 2i\omega B(s) y(s) + \bar{A}(s) y^2(s), \quad 0 \leq s \leq s_o, \tag{3.15}$$

subject to the initial condition $y(0) = 0$. Here $\bar{A}(s)$ denotes the complex conjugate of $A(s)$. Hence the solution can be expressed as

$$y(s_o) = -\int_0^{s_o} e^{-2i\omega \int_{s'}^{s_o} B(\xi)d\xi} A(s')ds' + E(s_o), \tag{3.16}$$

where the error term is

$$E(s_o) = \int_0^{s_o} \bar{A}(s') e^{-2i\omega \int_{s'}^{s_o} B(\xi)d\xi} y^2(s')ds'.$$

Set

$$v(s_o) = \sup_{0 \leq s \leq s_o} \left| \int_0^s e^{2iw \int_0^{s'} B(\xi)d\xi} A(s')ds' \right| \quad \text{and} \quad V(s) = \int_0^s |A(s')|\, ds'.$$

If $v(s_o)V(s) < 1$ then

$$|E(s)| \leq \frac{v^2(s_o)V(s)}{1 - v(s_o)V(s)}, \quad 0 \leq s \leq s_o. \tag{3.17}$$

Proof. Multiplying equation (3.15) by its integrating factor and integrating both sides from 0 to s, yields

$$\int_0^s e^{2i\omega \int_0^{s'} B(\xi)d\xi} y'(s')ds' + 2iw \int_0^s B(s') e^{2i\omega \int_0^{s'} B(\xi)d\xi} y(s')ds' =$$
$$-\int_0^s e^{2iw \int_0^{s'} B(\xi)d\xi} A(s')ds' + \int_0^s \bar{A}(s') e^{2i\omega \int_0^{s'} B(\xi)d\xi} y^2(s')ds'.$$

Consequently,

$$\int_0^s \frac{d}{ds'} \left(e^{2i\omega \int_0^{s'} B(\xi)d\xi} y(s') \right) ds' = e^{2i\omega \int_0^{s} B(\xi)d\xi} y(s)$$
$$= -\int_0^s e^{2i\omega \int_0^{s'} B(\xi)d\xi} A(s')ds' + \int_0^s \bar{A}(s') e^{2i\omega \int_0^{s'} B(\xi)d\xi} y^2(s')ds'. \tag{3.18}$$

Now solving for $y(s)$ and evaluating at $s = s_o$ in equation (3.18) we arrive at equation (3.16).

To achieve estimative (3.17) we start with

$$\begin{aligned} E(s) &= \int_0^s \bar{A}(s')e^{-2i\omega \int_{s'}^s B(\xi)d\xi} y^2(s')ds' \\ &= e^{-2i\omega \int_0^s B(\xi)d\xi} \int_0^s \bar{A}(s')e^{2i\omega \int_0^{s'} B(\xi)d\xi} y^2(s')ds'. \end{aligned}$$

Let

$$Y(s) = \int_0^s |A(s')|\,|y(s')|^2\,ds'. \tag{3.19}$$

Hence

$$|E(s)| = \left| \int_0^s \bar{A}(s')e^{2i\omega \int_0^{s'} B(\xi)d\xi} y^2(s')ds' \right| \le Y(s). \tag{3.20}$$

Differentiating equation (3.19) with respect to s,

$$Y'(s) = |A(s)|\,|y(s)|^2\,. \tag{3.21}$$

Note that from equations (3.16) and (3.20)

$$|y(s)| \le v(s_o) + Y(s), \quad 0 \le s \le s_o. \tag{3.22}$$

Thus substituting equation (3.22) into (3.21) leads to

$$Y'(s) \le |A(s)|\,(v(s_o) + Y(s))^2. \tag{3.23}$$

By integrating equation (3.23) from 0 to s, we obtain

$$\int_0^s \frac{Y'(s)}{(v(s_o) + Y(s'))^2} ds' \le \int_0^s |A(s')|\,ds' = V(s).$$

Therefore,

$$\frac{1}{v(s_o)} - \frac{1}{v(s_o) + Y(s)} \le V(s).$$

Thus if $v(s_o)V(s) < 1$, equation (3.20) gives

$$|E(s)| \le Y(s) \le \frac{v^2(s_o)V(s)}{1 - v(s_o)V(s)}, \quad 0 \le s \le s_o.$$

This concludes the lemma's proof. □

We now apply these results to our Ricatti equation. For brevity the argument T will be omitted in what follows. We apply the lemma above to the reflection kernel's problem (3.13)-(3.14) by letting $y(s) = \widehat{K}(x(s), \omega)$, $A(s) = \bar{\zeta}(x(s), \omega)$, $B(s) = \Gamma(x(s), \omega)$ and $s = x_o + X - x$, $s_o = X$. We deduce that

$$\widehat{K}(x, \omega) = -\int_x^{x+X} e^{2i\omega \int_{x'}^{x} \Gamma(s,\omega)\,ds} \bar{\zeta}(x', \omega)dx' + E(x, \omega), \tag{3.24}$$

with an error term given by

$$E(x,\omega)=\int_x^{x+X} e^{2i\omega\int_{x'}^{x}\Gamma(s,\omega)\,ds}\zeta(x',\omega)\widehat{K}^2(x',\omega)dx'.$$

Also

$$v(x_o,\omega)=\sup_{x_o\le x\le x_o+X}\left|\int_x^{x_o+X} e^{2i\omega\int_{x'}^{x_o+X}\Gamma(s,\omega)\,ds}\bar{\zeta}(x',\omega)dx'\right|$$

and

$$V(x_o,\omega)=\int_{x_o}^{x_o+X}|\zeta(x',\omega)|\,dx'.$$

Then in the cases where $v(x_o,\omega)V(x_o,\omega)<1$ the error bound follows.

Now we solve for $\widehat{R}(x_o,\omega)$ at an arbitrary point x_o by using equation (3.24) and (3.12) in equation (3.8). It results that

$$\widehat{R}_x(x,\omega)=\left(\zeta(x,\omega)\left(-\int_x^{x+X} e^{2i\omega\int_{x'}^{x}\Gamma(s,\omega)\,ds}\bar{\zeta}(x',\omega)dx'+E(x,\omega)\right)+\gamma\right)\ \widehat{R}(x,\omega).$$

Solving this initial value problem with $\widehat{R}(0,\omega)=\widehat{f}(\omega)$ then

$$\widehat{R}(x_o,\omega)=\widehat{f}(\omega)\ \exp\left[-\int_0^{x_o}\int_x^{x+X}\zeta(x,\omega)e^{2i\omega\ \int_{x'}^{x}\Gamma(s,\omega)\,ds}\ \bar{\zeta}(x',\omega)dx'+\gamma(x,\omega)\ dx\right]$$

$$\cdot\exp\left[\int_0^{x_o}\zeta(x,\omega)\ E(x,\omega)\,dx\right]. \tag{3.25}$$

For general rapidly varying orographies and $\beta<<1$ the error function $E(x,\omega)$ is small (see appendix C), even though the error estimate (3.17) is not useful in this case. It is sharp for instance when the function describing the medium properties (the metric coefficient $M(x)$ in system (2.1)) is taken to be piecewise constant on travel-time intervals with equal length (called a *Goupillaud medium*) [16].

Therefore, equation (3.25) leads to the *generalized O'Doherty-Anstey approximation*

$$\widehat{R}(x_o,\omega)\approx\widehat{f}(\omega)e^{-x_o(a_\beta(x_o,\omega)+b(x_o,\omega))}, \tag{3.26}$$

where

$$a_\beta(x_o,\omega)=\frac{1}{x_o}\int_0^{x_o}\int_x^{x+X}\zeta(x,\omega)e^{2i\omega\int_{x'}^{x}\Gamma(s,\omega)\,ds}\bar{\zeta}(x',\omega)dx'\,dx, \tag{3.27}$$

$$b(x_o,\omega)=-\frac{1}{x_o}\int_0^{x_o}\gamma(x,\omega)\,dx. \tag{3.28}$$

Using approximation (3.26) we can obtain an expression for $R(x_o,\tau)$ (the transmitted field in our applications) by using the Fourier inversion formula. Thus for $0\le\tau\le T$

$$R(x_o,\tau)\approx\frac{1}{2\pi}\int_{-\infty}^{\infty}\widehat{f}(\omega)e^{-x_o(a_\beta(x_o,\omega)+b(x_o,\omega))}e^{i\omega\tau}d\omega. \tag{3.29}$$

Note that the exponential factor in equation (3.29) accounts for the wave attenuation at travel time x_o. As mentioned above not always the error estimate given above is sharp. For this reason the error term $E(x_o,\omega)$ is calculated numerically in appendix C. Furthermore, for dispersion parameter β small enough and constant depth ($r(x)\equiv 0$) we have that $a_\beta = O(\beta^2)$ and $b = O(\beta)$. Hence for variable depths, it is reasonable to approximate the medium's dispersive correlation function $a_\beta(x_o,\omega)$ by the medium's hyperbolic correlation function $a_0(x_o,\omega)$, that is,

$$a_\beta(x_o,\omega) \approx \frac{1}{x_o}\int_0^{x_o}\int_x^{x+X} r(x)e^{2i\omega(x-x')}r(x')dx'\,dx \equiv a_0(x_o,\omega). \tag{3.30}$$

Moreover this hyperbolic version is easier to compute than the dispersive formula (3.27). Note that in the latter the function ζ depends on the frequency ω. Therefore the Fourier-type integral in a_β can not be computed rapidly by using the FFT (Fast Fourier Transform). On the other hand, the integral in equation (3.30) can be easily evaluated by the FFT algorithm because in this case the coefficient $r(x)$ is frequency independent. In appendix B we detail the numerical computation of the Fourier-type integral in coefficient $a_\beta(x_o,\omega)$. The accuracy of approximation (3.30) will be verified in section 4 showing that the leading order dispersive effects are controlled by coefficient $b(x_o,\omega)$.

The numerical experiments in section 4 will show that approximation (3.29) captures very well not only the wave front but also part of the forward scattering radiation. The parameter X in equation (3.27) (or (3.30)) regulates to what extent the incoherent signal is recovered.

If $\beta = 0$ then $b(x_o,\omega)\equiv 0$ and the approximation given by (3.26) reduces to

$$\widehat{R}(x_o,\omega) \approx \widehat{f}(\omega)e^{-x_o a_0(x_o,\omega)}, \tag{3.31}$$

where

$$a_0(x_o,\omega) = \frac{1}{x_o}\int_0^{x_o}\int_x^{x+X} r(x)e^{2i\omega(x-x')}r(x')dx'\,dx,$$

as in Berlyand and Burridge's work [3]. We recall that when $\beta\neq 0$ the hyperbolic medium's correlation function $a_0(x_o,\omega)$ (which controls the attenuation mechanism) is altered and an extra attenuation term $b(x_o,\omega)$ appears due to the model's dispersion.

4. Numerical validation of the generalized ODA theory. Consider the nonlinear terrain-following Boussinesq system deduced by Nachbin [18],

$$\begin{aligned} &M(\xi)\eta_t + \left(\left(1+\frac{\alpha\eta}{M(\xi)}\right)u\right)_\xi = 0,\\ &u_t + \eta_\xi + \frac{\alpha}{2}\left(\frac{u^2}{M(\xi)^2}\right)_\xi - \frac{\beta}{3}u_{\xi\xi t} = 0. \end{aligned} \tag{4.1}$$

We recall that when $\alpha = 0$ system (4.1) reduces to (2.1). Nevertheless for our numerical validation experiments we will use the nonlinear Boussinesq system in a small α regime. Two types of initial data are considered. We study the propagation of Gaussian-shaped disturbances of the form

$$u(\xi,0) = \eta(\xi,0) = e^{-(\xi-\xi_o)^2/\epsilon},$$

where the parameter ξ_o controls the pulse's initial position and $\epsilon > 0$ its effective width. Furthermore, we also consider solitary waves of the form

$$\begin{aligned}\eta(\xi,0) &= A_1 \ \mathrm{sech}^2(B(\xi-\xi_o)) + A_2 \ \mathrm{sech}^4(B(\xi-\xi_o)),\\ u(\xi,0) &= A \ \mathrm{sech}^2(B(\xi-\xi_o)),\end{aligned}$$

with A_1, A_2, A and B constants (to be defined in experiment 2). These are approximate solutions to system (4.1) with $M \equiv 1$ (see [23]).

Except in some special cases (for instance when $M \equiv 1, \alpha = 0$ or $\beta = 0$), finding the solution of system (4.1) is a nontrivial problem. To solve system (4.1) numerically we will use a finite difference solver introduced by Wei and Kirby [23]. This scheme will be used to perform numerical experiments in order to validate the theory developed in the previous sections.

First we rewrite system (4.1) in a more convenient way, as

$$\begin{aligned}\eta_t &= E(u,\eta),\\ V_t &= F(u,\eta),\end{aligned} \tag{4.2}$$

where

$$\begin{aligned}E(u,\eta) &= -\frac{1}{M(\xi)}\left(\left(1+\frac{\alpha\eta}{M(\xi)}\right)u\right)_\xi,\\ F(u,\eta) &= -\eta_\xi - \frac{\alpha}{2}\left(\frac{u^2}{M(\xi)^2}\right)_\xi,\end{aligned} \tag{4.3}$$

and V is an intermediate variable defined by

$$V = u - \frac{\beta}{3}u_{\xi\xi}.$$

To evaluate the boundary values we use the radiation conditions by Engquist and Majda [7]

$$\begin{aligned}u_t - u_\xi &= 0, \quad \text{at } \ \xi = \xi_{\text{min}},\\ u_t + u_\xi &= 0, \quad \text{at } \ \xi = \xi_{\text{max}},\end{aligned} \tag{4.4}$$

where ξ_{min} and ξ_{max} denote the left and right ends of the computational domain, respectively.

The evolution system above is solved by using an efficient predictor-corrector scheme. The $V \to u$ change of variables is done with an efficient (tridiagonal) ODE numerical scheme. Details, numerical properties and further numerical experiments are presented elsewhere [15, 16].

We now describe several experiments validating the dispersive pulse-shaping ODA theory.

Experiment set 1 (Flat channel and effectively linear regime): In these experiments the pulse is assumed to propagate over a flat bottom ($M \equiv 1$). In appendix A (c.f. equations (A.6) and (A.7)) we show that if in addition $\alpha = 0$ we can solve explicitly system (4.1) by using the Fourier transform technique. Flat channel solutions are employed to verify the numerical method's accuracy regarding dispersive and stability properties.

In figure 4.1 we see that the exact solution η (for $\alpha = 0$, $\beta = 0.03$) and the numerical solution (for $\alpha = 0.001$, $\beta = 0.03$) are in very good agreement at $t =$

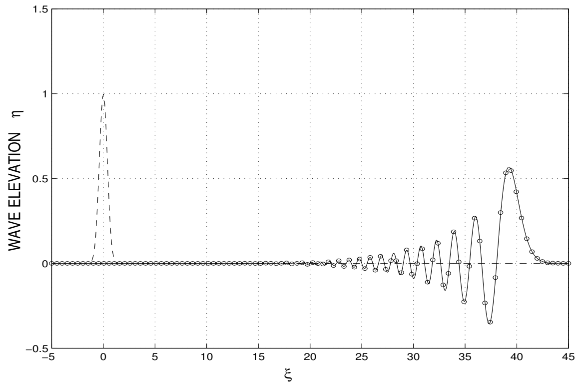

FIG. 4.1. *Dashed line: initial pulse* $\eta(\xi,0) = u(\xi,0) = e^{-\xi^2/0.3}$. *Solid line: numerical solution for* $\alpha = 0.001$, $\beta = 0.03$ *and* $t = 40$. *Dotted line: Exact solution.*

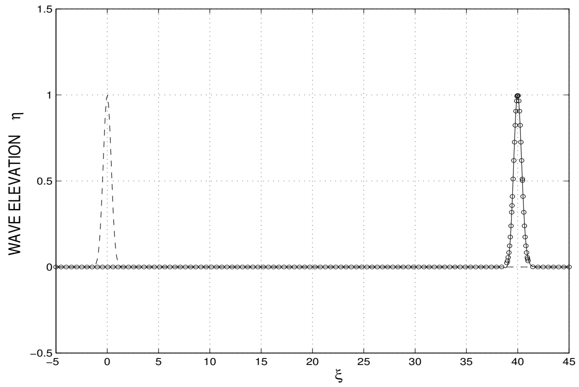

FIG. 4.2. *Dashed line: initial disturbance* $\eta(\xi,0) = u(\xi,0) = e^{-\xi^2/0.3}$. *Solid line: numerical solution for* $\alpha = 0.001$, $\beta = 0.0005$ *and* $t = 40$. *Dotted line: Initial Gaussian pulse translated to* $\xi = 40$.

40. After 40 length-units into the flat channel the right propagating Gaussian has developed an Airy-like oscillatory tail (c.f. appendix A). The dispersive properties of the numerical scheme are very good.

For this experiment the numerical parameters are $J = 4000$ (spatial mesh points; $\Delta\xi = 0.0125$) and $N = 5000$ (time mesh points; $\Delta t = 0.008$). As mentioned above, this test shows that the code is capturing very well the (effectively linear) dispersive regime when α is small enough.

We repeat the experiment above for $\alpha = 0.001$, $\beta = 0.0005$ and $t = 40$. Dispersion has been decreased substantially. Now the effective hyperbolic regime is clearly observed in figure 4.2.

Radiation conditions (4.4) also proved to absorb appropriately waves leaving the computational domain. It was observed that reflected waves produced by the computational boundaries were negligible.

Experiment 2 (Flat channel and weakly nonlinear regime/solitary wave): We now study system (4.1) in the case that $M \equiv 1$, $0 < \alpha << 1$ (weakly nonlinear regime), and $0 < \beta << 1$ (weakly dispersive regime). Under these hypotheses it is possible to obtain an approximate solution of system (4.1) which has the analytical

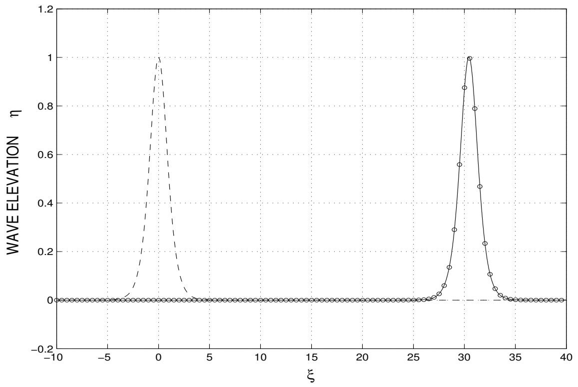

FIG. 4.3. *Solitary wave propagating over a flat bottom. Dashed line: initial disturbance* $\eta(\xi, 0) = A_1\ sech^2(B\xi) + A_2\ sech^4(B\xi)$. *Solid line: numerical solution for* $\alpha = 0.03$, $\beta = 0.03$ *and* $t = 30$. *Dotted line: Analytical solution (4.5).*

form

$$\begin{aligned} \eta(\xi, t) &= A_1\ \mathrm{sech}^2(B(\xi - Ct - \xi_o)) + A_2\ \mathrm{sech}^4(B(\xi - Ct - \xi_o)), \\ u(\xi, t) &= A\ \mathrm{sech}^2(B(\xi - Ct - \xi_o)), \end{aligned} \tag{4.5}$$

where

$$A_1 = \frac{C^2 - 1}{\alpha C^2} = \frac{1}{C^2}, \quad A_2 = \frac{(C^2 - 1)^2}{\alpha C^2} = \frac{\alpha}{C^2}, \quad C = \sqrt{1 + \alpha}, \quad A = \frac{C^2 - 1}{\alpha C} = \frac{1}{C},$$

and

$$B = \left\{ \frac{C^2 - 1}{(4/3)\beta C^2} \right\}^{1/2} = \left\{ \frac{\alpha}{(4/3)\beta C^2} \right\}^{1/2}.$$

Note that $A_1 + A_2 = 1$. See Wei and Kirby [23] for details.

In figure 4.3 we show the analytical solution η given by equation (4.5) for $\alpha = \beta = 0.03$ and $t = 30$. The initial soliton position is set to be $\xi_o = 0$. The numerical solution is also included in this plot. The numerical parameters are $J = 2000$, $N = 2500$, $\Delta\xi = 0.025$, $\Delta t = 0.012$. Note that we have the same dispersion level as in the first of Experiment set 1. Now weak nonlinearity prevents the formation of an oscillatory tail.

Observe that the pulse's propagation velocity is $C \approx 1.0149$, in agreement with solution (4.5). The code reproduces very well the weakly dispersive, weakly nonlinear evolution of the soliton.

Experiment set 3 (Disordered orography/Hyperbolic regime:) In experiments 1 and 2, in which the channel's bottom was assumed to be flat, the orography-dependent coefficient $M(\xi)$ was taken $M \equiv 1$. For variable depths the computation of function $M(\xi)$ involves the solution of a change of variables problem (conformal mapping) which is not an easy task. For this reason, in next experiments, the smooth orography coefficient $M(\xi)$ will be synthetized directly as a piecewise linear function, ignoring (for the time being) its dependence on the original orography. In [15] we describe in detail how a numerical conformal mapping tool [5] is used in order to obtain a "non-synthetic" $M(\xi)$. Nevertheless, synthetic $M(\xi)$ proves to be useful (i.e.

efficient) for observing the phenomena we are interested in and for validating the theory. The synthetized orography coefficient is conceived as

$$M(\xi) = 1 + \delta\mu(\xi/\ell),$$

where μ is a mean-zero coefficient constructed using a random number generator. The fluctuation level is indicated by δ and its correlation length by ℓ. In the following experiments we use $\delta = 0.5$ and $\ell = 0.1$.

The numerical experiments are performed over a channel defined in the interval [-15, 70]. The fluctuations of the synthetic coefficient $M(\xi)$ cover the interval [5, 45]. The data for the right propagating Gaussian is such that $\xi_o = -5$ and $\epsilon = 0.05$. The numerical solution is plotted as a function of the time-delay variable τ after propagating over 20 units of length and is presented in figure 4.4. Note the wave attenuation due to the orographic forcing. The transmited signal has amplitude 1.5 (smaller than 2.0, the initial amplitude). The agreement between the numerical solution of the full nonlinear equations (with small α) and the linear theory is very good (figure 4.4(b)). We also point out an outstanding feature of the theory, not noticed in previous work [3]. The linear hyperbolic ODA approximation is able to capture the forward scattering radiation, which is the incoherent coda behind the transmitted Gaussian. Theory and numerical experiment agree over the delay time interval up to $\tau = 10$ approximately.

To verify the robustness of the theory we increase the size of the disordered medium's slab used in the invariant imbedding theory (namely the variable X). In figure 4.4(c) we plot the same numerical solution as above but compared with a theoretical result using an increased slab size (up to $X = 20$). The approximate theory captures an even larger segment of the forward scattering radiation beyond $\tau = 15$.

Experiment set 4 (Disordered orography/Dispersive regime:) In the first experiment we consider the dispersion to be very weak ($\beta = 0.0005$). Figure 4.5(a) clearly shows that a very short oscillatory tail develops when the pulse propagates in a flat channel. The final amplitude of the transmitted pulse is about 1.5. The amplitude decay in this case is entirely due to dispersion as discussed in appendix A through the Airy kernel. But in the presence of orographic forcing an additional attenuation is observed (figure 4.5(b)). In this case the final amplitude is about 1. Note that no Airy-like oscillatory tail develops. This was systematically observed in several experiments and can be explained through the concept of *localization* [19]. The localization length of a Fourier mode is a *characteristic propagation distance* after which the transmission coeficient is negligible. The bulk of the energy is in the reflected signal. Moreover high frequency components have small localization lengths. This means they are quickly filtered (back) by the disordered medium. In the context of the ODA theory this was phrased in a slightly different way by Berlyand and Burridge [3]. They called a layered random medium a *stratigraphic Gaussian filter*. As presented here, the transmitted pulse can be written as the convolution of its initial Fourier content with a Gaussian kernel. The Gaussian kernel is the leading order approximation to the kernel in (3.29) with $\beta = 0$ (see [15, 16]). Applying this notion to our current problem we have that disorder filters the higher part of the Fourier content of the incoming pulse. Hence the oscillatory tail (which is of high frequency content) has been converted into the incoherent part of the wave. Again the agreement between the numerical solution and the ODA theory is very good.

In the next validation experiment the level of dispersion has been increased 4 times ($\beta = 0.002$). In figure 4.6(a) we have the initial pulse profile and the numerical

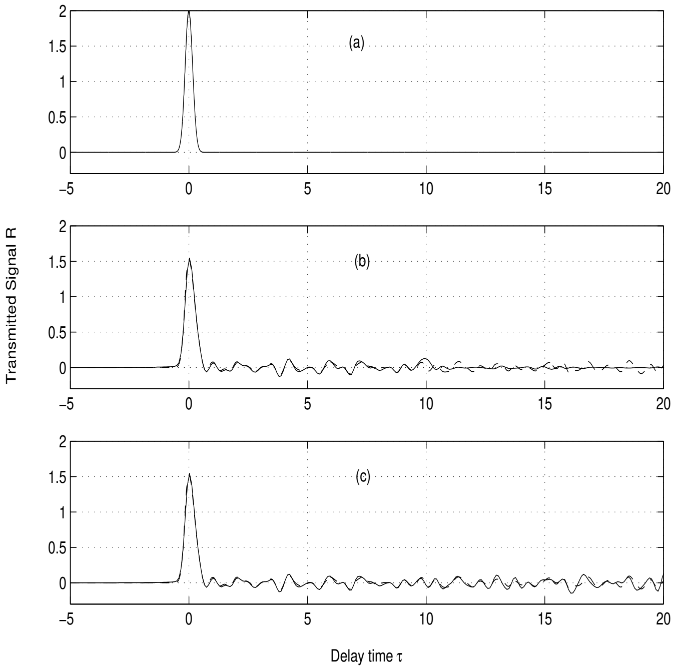

FIG. 4.4. *Pulse propagating over a synthetic disordered rapidly-varying topography. (a) Initial disturbance* $R(0,\tau) = 2e^{-\tau^2/0.05}$. *(b) Solid line: O'Doherty-Anstey approximation (3.31) for* $X = 5$. *Dashed line: Numerical solution for* $\alpha = 0.001$, $\beta = 0$ *at* $\xi = 20$. *(c) Solid line: O'Doherty-Anstey approximation (3.31) for* $X = 20$. *Dashed line: Numerical solution at* $\xi = 20$ *and* α, β *as in (b).*

solution after propagation over 40 units of a flat channel. We observe a long oscillatory tail due to the higher dispersion level.

To compute the theoretical ODA approximation we need the incoming pulse in time at the origin. Actually we need its Fourier content $\hat{f}(\omega)$. To be consistent with our mathematical theory we position the initial Gaussian profile (in space) to left of the origin at time t_o, allow it to propagate over a flat portion of the channel and record it in time at the origin. The starting time t_o is chosen so that the resulting pulse $f(\tau)$ be centered at $\tau = 0$. This gives us the correct incoming pulse (in time) for the theoretical formula to be used. Hence the incoming pulse displays a mild oscillatory tail as displayed by figure 4.6(a). In figure 4.6(b) we compare the numerical solution with the generalized ODA approximation. The dispersive wave attenuation can again be observed, in particular if we examine the envelop of the Airy-like solution.

Experiment 5 (Disordered orography/Solitary wave:) We are now in a position to explore the generalized ODA theory for a weakly nonlinear, weakly dispersive wave, namely a soliton. Using equations (4.5) it is easy to see that we have

$$f(\tau) = \left(\frac{1}{C^2} + \frac{1}{C}\right)\operatorname{sech}^2(B\tau) + \frac{\alpha}{C^2}\operatorname{sech}^4(B\tau),$$

in order to evaluate the ODA approximation (3.29).

We choose small values for the respective parameters $\alpha = \beta = 0.001$. Because the soliton is wider than the Gaussian (used before) we adopt $\ell = 0.6$. This keeps the wave/inhomogeneities ratio equal to approximately 10 as in all other experiments.

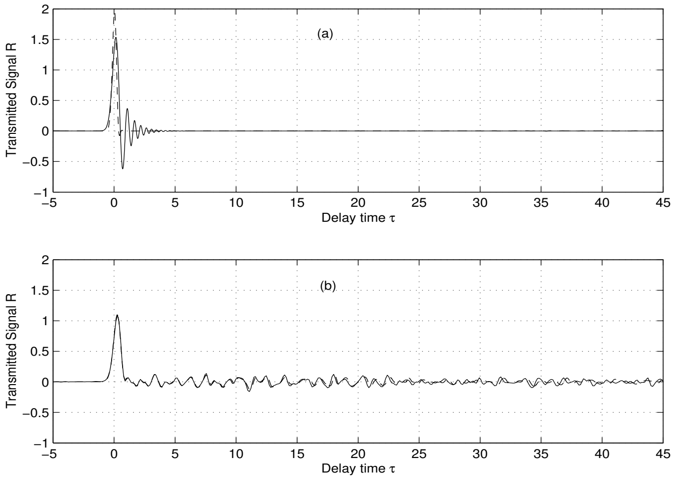

FIG. 4.5. *(a) Dashed line: Initial disturbance. Solid line: Solution for $M \equiv 1$ (flat bottom) at $\xi = 40$. (b) Pulse propagating over a synthetic disordered rapidly-varying orography. Dashed line: Numerical solution at $\xi = 40$. Solid line: Generalized O'Doherty-Anstey approximation (3.29) for $X = 20$. In all experiments $\alpha = 0.001$, $\beta = 0.0005$.*

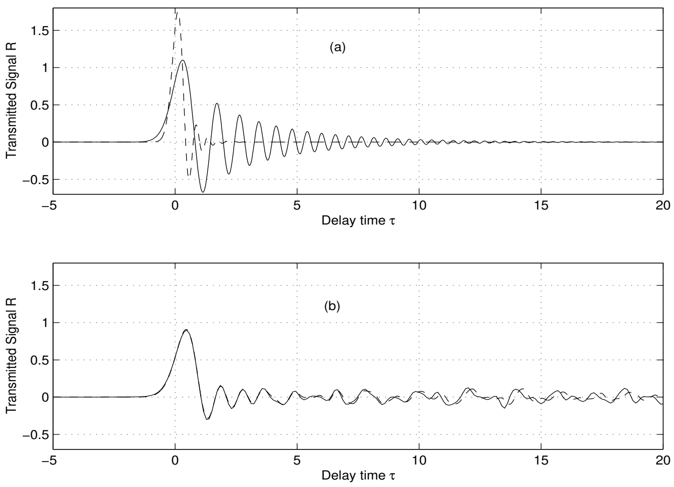

FIG. 4.6. *(a) Dashed line: Initial disturbance. Solid line: Solution for $M \equiv 1$ (flat bottom) at $\xi = 40$. (b) Pulse propagating over a synthetic disordered rapidly-varying orography. Dashed line: Numerical solution at $\xi = 40$. Solid line: Generalized O'Doherty-Anstey approximation (3.29) for $X = 20$. In all experiments $\alpha = 0.001$, $\beta = 0.002$.*

The orography coefficient covers the $[5, 245]$ interval and the amplitude of fluctuations is $\delta = 0.5$. In figure 4.7(b) we present the excellent agreement between the theory and the numerical solution.

More experiments with solitary waves, including time reversal and refocusing are presented in [15].

5. Conclusion and acknowledgements. We have formulated a generalization of the O'Doherty-Anstey theory for weakly dispersive waves. The theory has been valited numerically and pushed beyond its regime. In particular both the theoretical

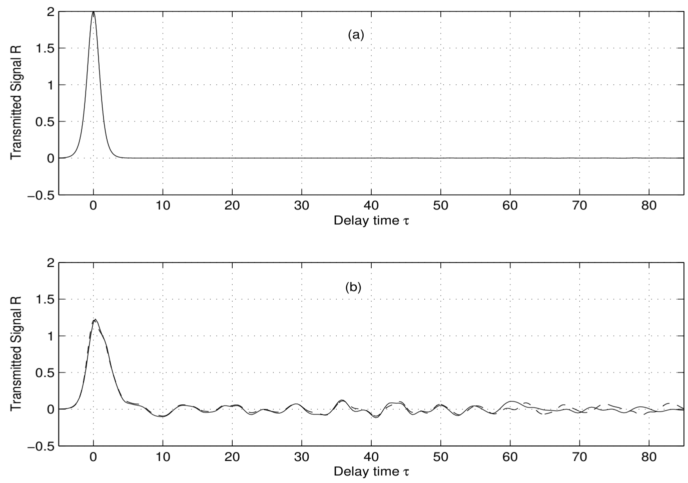

FIG. 4.7. *Soliton propagating over a synthetic disordered rapidly-varying orography. (a) Initial soliton $f(\tau)$. (b) Dashed line: Numerical solution for $\alpha = 0.001$, $\beta = 0.001$ at $\xi = 150$. Solid line: Generalized O'Doherty-Anstey approximation (3.29) for $X = 30$.*

expressions and the numerical experiments have been able to capture the apparent diffusion of small amplitude solitary waves. This is a theme of great interest: soliton propagation in disordered media. Further mathematical analysis is needed to fully understand this problem.

Part of this work was supported by NSF grant DMS97-09320 through the Mathematical Geophysics Summer Schools (1998–2002) at Stanford University. A. Nachbin is grateful to Prof. George Papanicolaou, as the MGSS Chairman, and for many useful discussions on this subject. Also to Prof. Robert Burridge for several helpful conversations regarding reference [3] during MGSS 1998.

Appendix A. Solutions for the linear KdV equation and the linear Boussinesq model.

The linear KdV equation

Consider the initial value problem

$$u_t + u_x + \gamma u_{xxx} = 0, \tag{A.1}$$
$$u(x,0) = f(x), \tag{A.2}$$

where γ is a nonzero constant. Using Fourier transform in x the solution for equations (A.1) and (A.2) is given by

$$u(x,t) = \frac{1}{2\pi}\int_{-\infty}^{\infty}\left(\int_{-\infty}^{\infty} e^{i(k(x-t-y)+\gamma k^3 t)}dk\right) f(y)dy. \tag{A.3}$$

Making a convenient change of variables, the inner integral in equation (A.3) can be expressed in terms of the Airy function to give

$$u(x,t) = \frac{1}{(3t\gamma)^{1/3}}\int_{-\infty}^{\infty} \mathrm{Ai}\left(\frac{x-t-y}{(3t\gamma)^{1/3}}\right) f(y)dy. \tag{A.4}$$

The Airy-kernel gives the rate in time at which a pulse $f(x)$ will spread due to dispersion. This is an useful information for the invariant imbedding technique used in the O'Doherty-Anstey theory.

The linear Boussinesq model

Now we study the linearization of system (4.1) for constant depth:

$$\begin{aligned} \eta_t + u_\xi &= 0, \\ u_t + \eta_\xi - \frac{\beta}{3} u_{\xi\xi t} &= 0, \end{aligned} \tag{A.5}$$

with the initial conditions

$$\eta(\xi,0) = u(\xi,0) = f(\xi).$$

Analogously to the KdV equation we can apply the Fourier transform technique to obtain the Fourier coefficients

$$\begin{aligned} \hat{\eta}(k,t) = \frac{\hat{f}(k)}{2} \Bigg[& \left(1 - \sqrt{1+(\beta/3)k^2}\right) e^{\frac{ikt}{\sqrt{1+\beta/3k^2}}} + \\ & \left(1 + \sqrt{1+(\beta/3)k^2}\right) e^{\frac{-ikt}{\sqrt{1+\beta/3k^2}}} \Bigg], \end{aligned} \tag{A.6}$$

$$\begin{aligned} \hat{u}(k,t) = \frac{\hat{f}(k)}{2\sqrt{1+(\beta/3)k^2}} \Bigg[& \left(1 + \sqrt{1+(\beta/3)k^2}\right) e^{\frac{-ikt}{\sqrt{1+\beta/3k^2}}} \\ & - \left(1 - \sqrt{1+(\beta/3)k^2}\right) e^{\frac{ikt}{\sqrt{1+\beta/3k^2}}} \Bigg]. \end{aligned} \tag{A.7}$$

We point out that in the hyperbolic case ($\beta = 0$) the above initial data gives rise to (only) a right propagating mode. In the dispersive case a negligible left propagating mode is always present in this type of data. Notice that because of (A.6), (A.7) and

$$\frac{1}{\sqrt{1+(\beta/3)k^2}} = 1 - (k^2/6)\beta + O(\beta^2),$$

we have that

$$\widehat{L}(t,k) = \hat{\eta}(t,k) - \hat{u}(t,k) = O(\beta) \approx 0,$$

provided that β is small enough. For the hyperbolic case the left propagating mode is identically zero.

The dispersion relation for system (A.5) is

$$\omega_\pm = \omega_\pm(k) = \pm \frac{k}{\sqrt{1+\frac{\beta}{3}k^2}}, \tag{A.8}$$

where ω_+ and ω_- represent Fourier modes propagating to the right and left, respectively. In opposition to the KdV equation the phase velocity is

$$C_k^\pm = \frac{\omega_\pm}{k} = \pm \frac{1}{\sqrt{1+\frac{\beta}{3}k^2}},$$

which does not switch signs and is bounded by one. Furthermore, $\omega_+ = \omega_+(k)$ coincides up to $O(k^3)$ with the dispersion relation for the KdV equation above with $\gamma = \beta/6$. Note also that, for waves generated in space, the range of possible time frequencies is bounded by $(3/\beta)^{1/2}$ for all k. As a consequence, solutions u, η of system (A.5) are band-limited functions in t. This fact justifies why frequencies ω higher than $\sqrt{3/\beta}$ are not considered in the analysis presented in section 3.

Appendix B. Numerical computation of coefficients $a_\beta(x_o, \omega)$ and $b(x_o, \omega)$. As mentioned in section 3, the numerical computation of the dispersive coefficient $a_\beta(x_o, \omega)$ is expensive. To override this difficulty we approximated it by the hyperbolic medium's correlation function $a_0(x_o, \omega)$, which corresponds to the leading order term of a Taylor series expansion of a_β around $\beta = 0$. The numerical experiments in section 4 showed the high accuracy of this approximation.

To compute coefficient $a_0(x_o, \omega)$ as in equation (3.30) we rewrite it as

$$a_0(x_o, \omega) = \int_0^X \Phi(\eta) e^{-2i\omega\eta} d\eta, \tag{B.1}$$

where

$$\Phi(\eta) = \frac{1}{x_o} \int_0^{x_o} r(x) r(x + \eta) dx.$$

We know by the correlation theorem that

$$\int_{-\infty}^{\infty} r(x) r(x + \eta) dx = F^{-1}[\hat{r}\overline{\hat{r}}](\eta),$$

where the hat denotes the Fourier transform, F^{-1} the inverse Fourier transform and the bar indicates complex conjugation. Therefore function Φ defined above can be computed by using the FFT algorithm letting the coefficient $r(x)$ be zero outside the interval $[0, x_o]$. This is consistent with the invariant imbedding approach. We must append enough zeros to the tail of the sampled coefficient $r(x)$ (zero padding) in order to eliminate the overlapping phenomenon that appears due to the fact that $r(x)$ is not a periodic function. The Fast Fourier transform (FFT) assumes periodicity in both physical and frequency domains (see Brigham [4]). The cost of computing the discrete correlation function results in only three FFT evaluations which is faster than an ordinary computation of the integral defining Φ for each value of η. The numerical code to perform the discrete correlation can be found in [4].

Once the function Φ is known, the windowed Fourier transform in equation (B.1) is evaluated by using only one FFT. Analogously to the discrete correlation zero padding outside the inverval $[0, X]$ is required on the sampling of function Φ.

To evaluate the generalized O'Doherty-Anstey approximation presented in section 3 we also need the dispersive coefficient $b(x_o, \omega)$. To make its computation faster we rewrite it in the more compact form

$$b(x_o, \omega) = -\frac{\beta}{6x_o} \int_0^{\xi(x_o)} \frac{-i\omega^3 M^{3/2}(\xi) + M'(\xi)\omega^2}{1 - (\beta/3)M(\xi)\omega^2} d\xi, \tag{B.2}$$

where the upper limit $\xi(x_o)$ denotes the spatial position in the medium corresponding to the travel time x_o. Thus we must compute only once the coefficients $M(\xi)$, $M^{3/2}(\xi)$

and $M'(\xi)$ which can be stored at the beginning. The integral in (B.2) is approximated by the trapezoidal method for roughly 2^{14} frequencies in the range $|\omega| < C_o(x_o)\sqrt{3/\beta}$. Since $b(x_o, -\omega) = \overline{b(x_o, \omega)}$ only positive frequencies must be evaluated.

Appendix C. Error Estimation of the Pulse-Shaping Theory.

In section 3 the reflection kernel K was decomposed according to the result of the lemma presented. In the derivation of the generalized ODA approximation (under the hypotheses of rapidly-varying orography and weakly dispersive regime $0 < \beta << 1$) we retained only the first term on the right handside of the decomposition leading to the approximation

$$\widehat{K}(x,\omega) \approx -\int_x^{x+X} e^{2i\omega \int_{x'}^{x} \Gamma(s,\omega)\,ds}\bar{\zeta}(x',\omega)dx'. \tag{C.1}$$

We wish to give numerical evidence showing the accuracy of this approximation. First of all, observe that the reflection kernel K can be computed by solving numerically the Ricatti equation

$$\widehat{K}_x = \bar{\zeta}(x,\omega) + 2i\omega\Gamma(x,\omega)\widehat{K} - \zeta(x,\omega)\widehat{K}^2,$$

subject to

$$\widehat{K}(x_o + X, \omega; T) = 0.$$

See definitions of coefficients Γ and ζ in section 3. Consequently, we can evaluate the error function $E(x_o, \omega)$ at any time x_o and frequency ω. The results are presented in figure C.1 where we compare the norm of function $E(x_o, \omega)$ to that of approximation (C.1) at point $\xi = 40$, with $X = 20$ and $\beta = 0.005$. We see that the error function results negligible for all frequencies. The parameters used for the orography considered here are $L = 240$ (total length of the rough bottom), $\ell = 0.6$ (scale of variation of the orography) and $\delta = 0.5$ (amplitude of orography's fluctuations).

REFERENCES

[1] M. Ash, W. Kohler, G. C. Papanicolaou, M. Postel and B. White, *Frequency content of randomly scattered signals*, SIAM Review, V 33, (1991) pp. 519-625.

[2] P.G. Baines, *Topographic Effects in Stratified Flows*, Cambridge Univ. Press, 1995.

[3] L. Berlyand and R. Burridge, *The accuracy of the O'Doherty-Anstey approximation for wave propagating in highly disordered stratified media,* Wave Motion 21 (1995), pp. 357-373.

[4] E.O. Brigham, *The Fast Fourier Transform and its Applications.* Prentice Hall, 1988.

[5] T. Driscoll, http://www.math.udel.edu/driscoll/software.

[6] European Centre for Medium-Range Weather Forecasts (ECMWF), *Orography*, Proceedings of a Workshop held at ECMWF, 1998.

[7] B. Engquist and A. Majda, *Absorbing boundary conditions for the numerical simulation of waves,* Math. Comp., 31 (139) (1977), pp. 629-651.

[8] J.F. Clouet and J. P. Fouque, *Spreading of a pulse travelling in random media.*, Annals of Applied Probability, V 4, (1994) pp. 1083-1097.

[9] J. Hamilton, *Differential equations for long-period gravity waves on a fluid of rapidly vaying depth,* J. Fluid Mech., 83 (1977), pp. 289-310.

[10] P. Lewicki, R. Burridge and M. de Hoop, *Beyond effective medium theory: Pulse stabilization for multimode wave propagation in high-contrast layered media,* SIAM J. Appl. Math., 56, No. 1 (1996), pp. 256-276.

[11] F. Mattioli, *Decomposition of the Boussinesq Equations for Shallow-Water into a set of Coupled Korteweg-de Vries Equations,* Phys. Fluids A 3 (10) (1991), pp. 2355-2359.

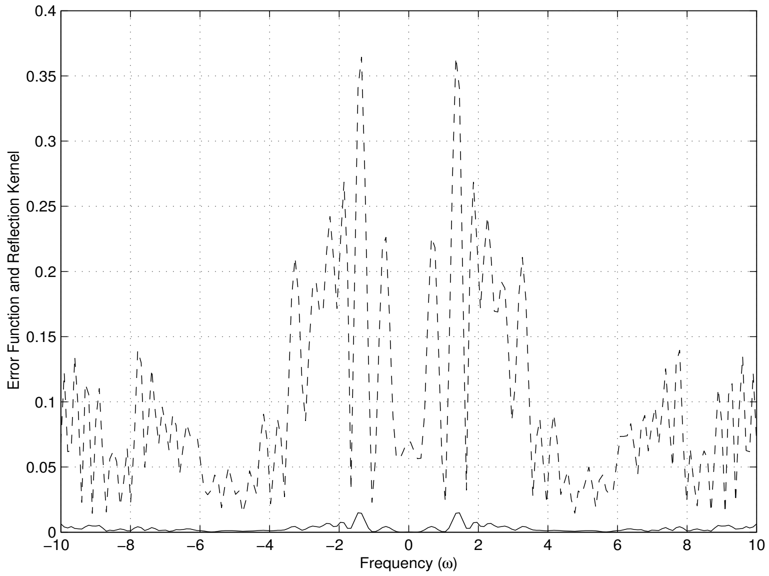

FIG. C.1. *Solid line: Error's norm for $\beta = 0.005$, $X = 20$ at $\xi = 40$. Dashed line: Norm of approximation (C.1) for the same parameters.*

[12] F. MATTIOLI, *On the Hamiltonian Decomposition of the Boussinesq Equations in a pair of Coupled Korteweg-de Vries Equations,* Wave Motion, 28 (1998), pp.283-296.

[13] C.C. MEI, *The Applied Dynamics of Ocean Surface Waves*, (1983) John Wiley.

[14] G. MEYER, *Initial Value Methods for Boundary Value Problems: Theory and Application of Invariant Imbedding*, Academic Press, 1973.

[15] J.C. MUÑOZ GRAJALES AND A. NACHBIN, *Dispersive pulse stabilization and solitary wave refocusing*, in preparation, 2002.

[16] J. C. MUÑOZ GRAJALES, *Dispersive wave attenuation and refocusing due to disordered orographic forcing*, PhD thesis (in english), IMPA, Brazil, 2002.

[17] A. NACHBIN, *Modelling of Water Waves in Shallow Channels.* Computational Mechanics Publications, Southampton, U.K., 1993.

[18] A. NACHBIN, *A terrain-following Boussinesq system*, to appear SIAM Appl. Math., 2002.

[19] A. NACHBIN, *The localization length of randomly scattered water waves,* J. Fluid Mech., 296 (1995), pp. 353-372.

[20] R.F. O'DOHERTY AND N. A. ANSTEY, *Reflections on amplitudes*, Geophysical Prospecting, V. 19, (1971) pp. 430-458.

[21] D. H. PEREGRINE, *Long waves on a beach,* J. Fluid Mech., 27 (1967), pp. 815-827.

[22] G. PAPANICOLAOU AND K. SØLNA, *Ray theory for a locally layered random medium*, Waves in Random Media, V. (2000) pp. 151-198.

[23] G. WEI AND J. KIRBY, *Time-Dependent Numerical Code for Extended Boussinesq Equations,* J. of Waterway, Port, Coastal, and Ocean Engineering, Vol. 121, No. 5 (1995), pp. 251-261.